Localized excited states observed in superconducting quench-condensed and annealed manganese-doped zinc films

B. D. Terris* and D. M. Ginsberg
Department of Physics and Materials Research Laboratory, University of Illinois at Urbana—Champaign, Urbana, Illinois 61801
(Received 31 May 1983; revised manuscript received 13 October 1983)

We have measured the electron-tunneling characteristics of a dilute, superconducting zinc-manganese alloy, both for a quench-condensed thin film and for one annealed at room temperature. The ac-conductance curve of the annealed film showed a well-defined structure in the energy gap corresponding to localized states predicted by the theory of Shiba and Rusinov or that of Müller-Hartmann and Zittartz. The observed band was broader than predicted. The ac conductance of the quench-condensed film showed an even broader structure. The annealed film's density of states at zero energy agreed reasonably well with that calculated from critical-field measurements of Smith on bulk Zn-Mn.

I. INTRODUCTION

In previous papers[1–3] our group has reported the electron-tunneling observation of localized states associated with the presence of magnetic atoms in quench-condensed superconducting thin films. In all of those experiments, the dopant atoms were insoluble in the host metal, so the measurements were made only on quench-condensed films. Another way of overcoming the solubility problem is to use ion-implanted samples, as shown by Bauriedl *et al.*[4] Both of these methods, quench condensation and ion implantation, suffer from the disadvantage that disorder is introduced into the sample, so it may differ from bulk material.

It is believed that small concentrations of manganese are soluble in zinc at low temperatures.[5] Measurements by Falke *et al.*[6] indicate that the addition of Mn to Zn causes a depression of the transition temperature which is nearly the same for quench-condensed films, annealed films, and bulk samples. Therefore, Zn-Mn may be a system in which it is possible to make useful tunneling measurements on both quench-condensed and annealed thin-film samples, and it may be useful to compare the results with thermodynamic data found in the literature for bulk samples.[7]

The value for the initial depression of the transition temperature in thin films[6] of Zn-Mn is 285 K/at.%, which is higher than that found for any other system. The size of this effect indicates that the exchange interaction between the magnetic atoms and the conduction electrons is unusually strong in Zn-Mn, compared to that in other superconductors doped with magnetic atoms.

We have therefore measured the tunneling characteristics of quench-condensed and annealed thin films of Zn doped with 1 at. ppm Mn. Previous tunneling measurements[1–4] of other alloys showed a structure associated with the magnetic atoms below the main rise in the I-V and dI/dV characteristics of superconductor-insulator-superconductor (SIS) tunnel junctions. We have observed a similar structure for quench-condensed Zn-Mn (1 at. ppm) films, and have observed a much sharper structure of the same type for annealed Zn-Mn (1 at. ppm) films. We have also compared our results with critical field data on bulk samples[7] and have found reasonably good agreement.

Shiba's theory[8] (equivalent to Rusinov's theory[9]) predicts that the exchange interaction between the conduction electrons and the magnetic atoms will generate a band of states in the BCS energy gap, located around an energy $\epsilon_l\Delta$ for each value of the orbital angular momentum l,[10] where Δ is the superconducting order parameter. The values of the ϵ_l's depend on the strength of the exchange interaction. In previous papers[1–3] contributions from s, p, and d waves ($l=0,1,2$) were included, and the values of ϵ_l which had been calculated from band theory[11] produced a good fit to the tunneling data. We have also found it necessary to include s-, p-, and d-wave scattering in order to obtain a good fit to our Zn-Mn data, but in this case the ϵ_l's found from band theory do not produce a good fit.

II. EXPERIMENTAL METHOD

A master alloy of zinc with 10 000 at. ppm manganese was prepared from 0.1037 g of 99.9%-pure Mn (Ref. 12) and 12.153 g of >99.999%-pure Zn.[13] The Zn and Mn metals were etched in HCl before being used. The metals were sealed in a Pyrex tube (11 mm inner diameter), which had been evacuated to a pressure of less than 10^{-5} Torr. The sealed tube was placed in a 450 °C oven. To ensure homogeneity of the alloy, the tube was shaken about every half hour. After 5 h, the tube was removed from the oven and cooled in a stream of air while being shaken. It was then placed in an oven at 400 °C (below the melting point) for one half hour. The oven was then shut off and left closed in order to cool slowly. (The manganese is soluble in Zn above room temperature.[5]) Once cool, the tube was broken open and the alloy was removed. After etching the alloy in HCl, it was pressed thin. The master alloy was then diluted, following the same procedure, to produce a 100-at. ppm alloy, which was further diluted to produce a 1-at. ppm alloy. The 1-at. ppm alloy was later cut into pellets for flash evaporating. A pure Zn ingot was simi-

larly prepared and was used to make a sample for comparison.

Prior to etching the 10 000-at. ppm alloy, a piece of it was analyzed by optical and scanning electron microscopy.[14] Regions of pure Zn and eutectic Zn-Mn were found distributed uniformly throughout the bulk of the sample. A Mn-rich surface layer was also found. We concluded that after etching the surface layer, we were left with an alloy that was uniform on a macroscopic scale, so small pieces of the bulk would be identical to one another in composition.

The tunnel junctions were fabricated by first evaporating three aluminum films onto a glass substrate. The films were then exposed to air for ~ 1 h in order to form an insulating aluminum oxide barrier on each film, and the substrate was placed into a ^{4}He cryostat. After evacuating the cryostat to a pressure of less than 5×10^{-6} Torr and cooling the substrate to 1.1 K, a Zn-Mn (or Zn) film was deposited onto it by quickly evaporating alloy pellets. The pellets were dropped, a few at a time, into a room-temperature tungsten boat (0.051 mm thick), which was then slowly heated to 1200 °C (as measured by an optical pyrometer). The evaporation of each pellet added about 10 Å to the film thickness. The boat was then cooled and more pellets were dropped. This procedure was adopted because pellets dropped into a 1200 °C boat were carried off under their own vapor pressure before completely evaporating. (Prior to dropping the first pellets, the boat had been outgassed at 1200 °C.) The sample was then held below 4.2 K while tunneling data were taken. When taking these data, the earth's magnetic field was canceled to better than 15 mG.

We also desired to study the properties of annealed Zn-Mn films. Since annealed Zn films have a superconducting transition temperature (T_c) below the lowest temperature obtainable with a ^{4}He cryostat, we needed to warm up the sample and transfer it to a ^{3}He system. This could be done because Mn is soluble in Zn at the desired concentration at room temperature.[5] The cryostat was slowly warmed to room temperature (in ~ 2 d), and SiO was evaporated onto the junctions. (We found that exposure to oxygen destroyed the junctions.) The cryostat was then opened and the substrate was transferred to a ^{3}He system. The substrate was then cooled to ~ 0.4 K and data were taken.

Two successful sets of tunnel junctions were made with Zn doped with 1 at. ppm Mn, and one set with pure Zn. Their I-V and (dI/dV)-V characteristics were measured before and after annealing. The I-V characteristics were measured by biasing the junction with a low-impedance voltage source and simultaneously measuring the circuit's current and the voltage across the junction. The dI/dV curve was obtained by imposing a small ($\lesssim 25$ μV peak-to-peak) ac signal (500 or 1000 Hz) onto the dc voltage. The component of the measured current at the fundamental frequency was then proportional to dI/dV. In each run, all three junctions showed nearly identical characteristics. We show here the results from one doped and one pure junction.

III. RESULTS

Shown in Table I are characteristics of the two junctions discussed here. T_{c1} is the temperature at which the sample film (quench-condensed or annealed) reached 50% of its normal-state resistance in a four-terminal measurement. δT_{c1} is the transition width of the sample film, defined as the temperature change required to increase the film's resistance from 10% to 90% of its normal-state resistance. All of the temperatures in this paper refer to the T_{58} temperature scale.

In the quench-condensed as well as the annealed samples, we found that the values of T_c for Zn and Zn-Mn were sample dependent. In Table II, we show T_c for all of our quench-condensed samples. All of the T_c's for Zn-Mn are lower than all of those for the pure Zn, although there is a wide range of values in both cases. We also note that our T_c's for the annealed samples were higher than the value for bulk Zn, 0.885 K, reported in the literature.[15]

The experimental normalized conductances for the pure Zn sample and the Zn doped with 1 at. ppm Mn sample are shown by the solid lines in Fig. 1. We discuss the conductance curves in terms of Δ_1 and Δ_2, the superconducting order parameter of the sample film and the aluminum counterelectrode, respectively. (For the very low level of doping which we have used, the order parameter and the width of the energy gap are very nearly the same.) In the doped sample, there is a bump in the conductance centered at $V\cong 0.275$ mV, and a small rise just below

TABLE I. Zn and Zn-Mn sample characteristics.

Sample material	c (at. ppm)	Sample thickness (Å)	Counter-electrode thickness (Å)	SiO thickness (Å)	Sample phase	T_{c1} (K)	δT_{c1} (K)	Junction resistance (kΩ)
Zn	0	192±17	637±47	1454±111	quench-condensed	1.524 ±0.01	0.126	0.71±0.01
					annealed	1.060 ±0.01	0.060	1.07±0.01
Zn-Mn	1	155±18	536±76	750± 50	quench-condensed	1.442 ±0.01	0.129	7.38±0.08
					annealed	0.969 ±0.01	0.043	7.49±0.08

TABLE II. T_c of quench-condensed Zn and Zn-Mn films.

T_c(Zn) (K)	T_c(Zn-Mn) (K)
1.556	1.271
1.599	1.411
1.565	1.385
1.524	1.358
	1.442
	1.515

$V \cong 0.20$ mV. As will be shown, these two structures are associated with the Mn atoms in the Zn. In addition to these two structures, the expected cusp at $|\Delta_1 - \Delta_2|/e \cong 0.06$ mV and the main peak at $(\Delta_1 + \Delta_2)/e \cong 0.38$ mV, there is a secondary peak in both junctions at a voltage greater than $(\Delta_1 + \Delta_2)/e$. This peak is due to a thin edge of the aluminum film, which has a larger energy gap than the rest of the film.[16] A two-terminal resistance measurement of the aluminum film's T_c gives a value of Δ_2. This value is too large (by $\sim 20\%$) to be consistent with that determined from the tunneling curve, indicating that part of the film has a larger energy gap than the remainder of the film. (Our second doped sample showed a much smaller edge-effect peak, but similar Mn-associated structure. However, for this sample

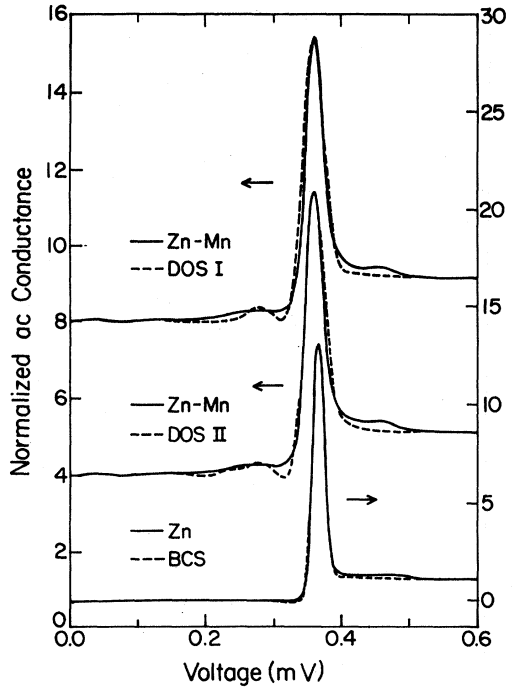

FIG. 1. Solid curves show the experimental normalized ac conductances at $T = 0.367$ K for the annealed, Zn-Mn (1 at. ppm) sample (upper two curves) and the pure Zn sample (lowest curve). The dashed lines next to the top and middle curves show the theoretical conductances generated from DOS I and DOS II of Fig. 4, respectively. The dashed line next to the bottom curve shows the ac conductance generated from a BCS DOS. The upper two sets of curves have been offset vertically for clarity.

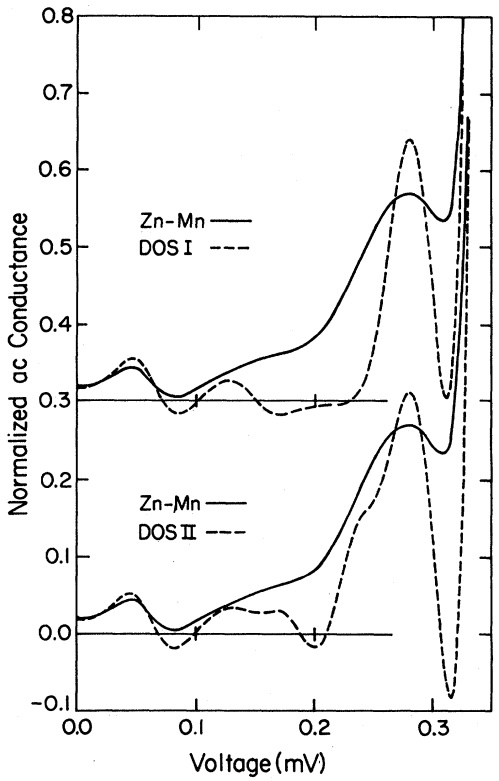

FIG. 2. Low-bias-voltage region of the upper two sets of curves shown in Fig. 1. The upper set has been offset vertically for clarity.

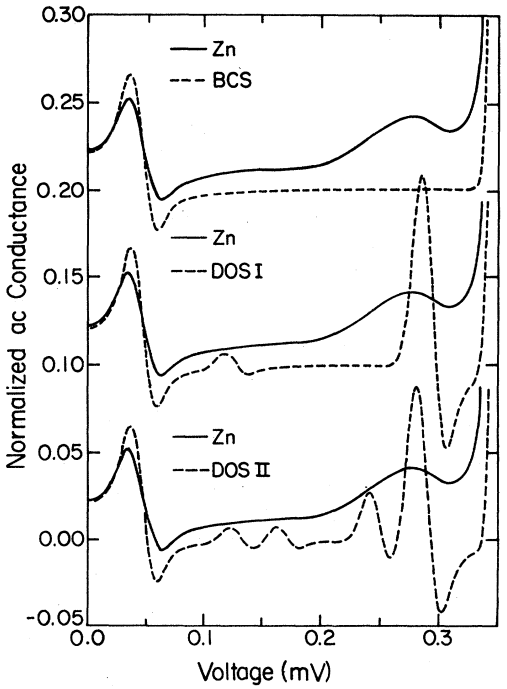

FIG. 3. Solid curves show the low-bias-voltage region of the ac conductance for the annealed pure Zn sample. The dashed lines show the ac conductances calculated from a BCS DOS (top curve), from the set of ϵ_l's used in DOS I of Fig. 4 (middle curve), and from the set of ϵ_l's used in DOS II of Fig. 4 (bottom curve). The upper two sets of curves have been offset vertically for clarity.

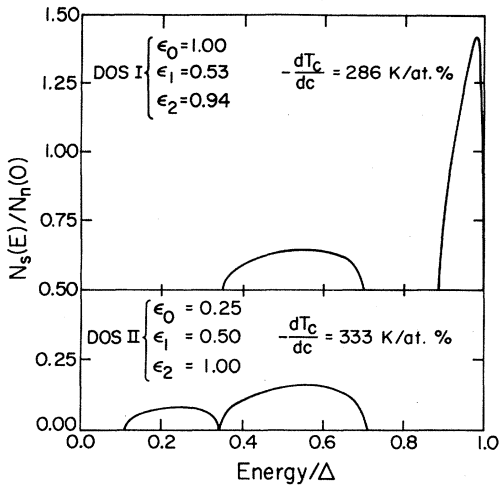

FIG. 4. The two DOS for Zn-Mn, as a function of energy, calculated using Shiba's theory for two sets of ϵ_l's. The upper DOS has been shifted up by one-half unit for clarity.

there was some uncertainty in the temperature at which the tunneling data were taken.)

We have compared our measured ac conductances with those predicted by BCS and by Shiba.[8] These conductances are shown in Fig. 1, and the low bias regions are shown in Figs. 2 and 3 on expanded scales. The lower curve in Fig. 1 and the upper curve in Fig. 3 show the measured normalized conductance for pure Zn, and the dashed lines next to them show the conductance calculated from a BCS density of states. The upper two curves in Fig. 1 and the two curves in Fig. 2 show the conductance of the doped sample along with the conductance calculated from two different Shiba-type densities of states (DOS). These two DOS, as shown in Fig. 4, were calculated from Shiba's theory, as described in Ref. 1. The upper DOS in Fig. 4, corresponding to the upper fit to the doped-sample data in Figs. 1 and 2, was calculated by using just one band of states at the position of the main Mn-associated bump (at $V=0.275$ mV). It is seen that the small rise in the conductance below $V=0.20$ mV would be attributed to the thermally excited quasiparticles occupying this one band in the DOS. The best fit using one band was obtained for $\epsilon_1=0.53$. An equivalent fit can be obtained by using s-wave (ϵ_0) instead of p-wave (ϵ_1) scattering, but in order to have the same size structure in the DOS, the concentration used in the calculation would have to be increased by a factor of $(2l+1)=3$ and would no longer agree well with the experimental value. The value of ϵ_2 was chosen so that the predicted initial depression of T_c with Mn concentration, dT_c/dc, would agree with the experimental value for thin films 285±30 K/at.%.[6] We used the relation[11]

$$dT_c/dc = -\sum_l (2l+1)(1-\epsilon_l^2)/8kN_n(0)\ ,$$

where $N_n(0)=0.139$ states/eV atom as determined from specific heat measurements.[17] Choosing $\epsilon_2=1.0$ gives an almost identical conductance.

An attempt to obtain better agreement between theory and experiment was made by using two bands, s wave and p wave. The second curve for the doped sample shown in Figs. 1 and 2 was calculated from the second DOS shown in Fig. 4. This curve gives a slightly better fit to the data than that calculated from the first DOS, but there is still a significant difference between theory and experiment. The predicted dT_c/dc for the second DOS is also in good agreement with experiment, as is the concentration used. Some other choices for the ϵ_l's would also match the observed structure and the value for dT_c/dc.

In the pure Zn conductance curve shown in Fig. 3, there is a small bump. This might be a sign that the "pure" Zn contains a magnetic impurity. Since the bump in Fig. 3 occurs at about the same voltage as the one in Fig. 2, we tentatively ascribe it to a small concentration of Mn. We have used the two sets of ϵ_l's from Fig. 4 in order to estimate this Mn concentration, and we show the fits in the bottom two curves of Fig. 3. By approximately matching the area of the theoretically calculated band of states to that observed, we estimate the concentration of Mn in our pure Zn to be ~0.1 at. ppm. It is possible that our pure Zn had such a concentration of Mn impurities.

We notice that the pure- and doped-sample conductances also differ in the height of the main peak at $(\Delta_1+\Delta_2)/e$, as can be seen in Fig. 1. This difference is consistent with the theoretical prediction that the addition

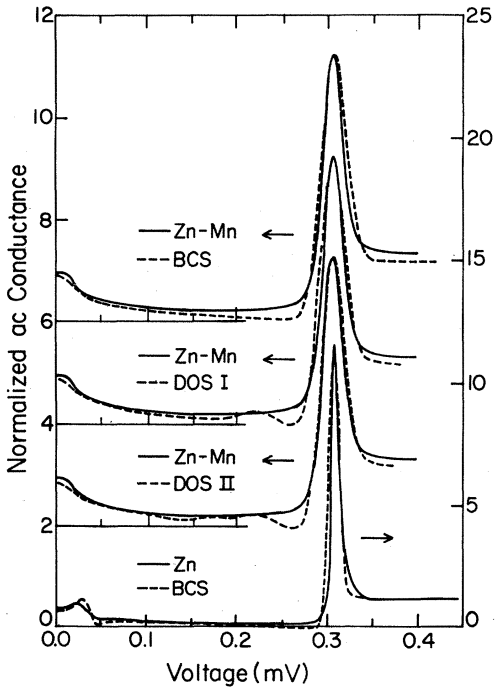

FIG. 5. Solid curves show the experimental normalized ac conductance for the quench-condensed Zn-Mn (1 at. ppm) sample at $T=1.09$ K (upper three curves) and for the quench-condensed pure Zn sample at $T=1.07$ K (bottom curve). The dashed lines next to the top and bottom curves are the ac conductances generated from a BCS DOS. The dashed lines next to the second and third curves are the ac conductances generated from DOS I and DOS II of Fig. 4, respectively. The upper three sets of curves have been offset vertically for clarity.

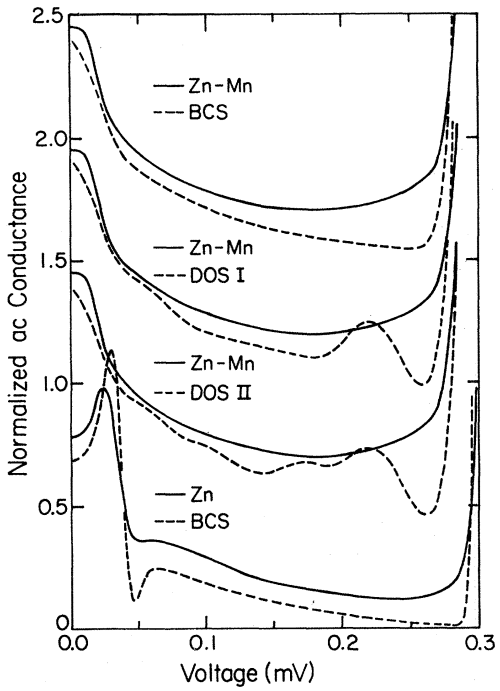

FIG. 6. Low-bias-voltage region of the curves shown in Fig. 5. The upper three sets of curves have been offset vertically for clarity.

of magnetic atoms to the superconducting host will lower and round the peak in the DOS at the gap edge. It is possible, however, that the difference is due to differences in junction quality and is not related to the Mn doping.

Falke *et al.*[6] have found that dT_c/dc for quench-condensed Zn-Mn films is almost identical to that for bulk samples, to within the accuracy of their experiment. This suggests that the effect of Mn in quench-condensed and annealed Zn is the same, and that the two may have the same DOS. However, we find that is not true. Shown by the solid lines in Fig. 5 and 6 are the normalized conductances of the quench-condensed samples. Along with the data for the pure Zn sample (lowest curve), we show the BCS conductance. The data for the doped sample are shown in the upper three curves. The upper doped-sample curve is plotted along with the predicted BCS conductance, and the lower two doped-sample curves are shown with the conductances calculated using the same sets of ϵ_l as in Fig. 4. We note that just before the main peak there is a small rise in the doped sample that is not present in the pure sample. The two DOS of Shiba give better fits to the doped data than does BCS, but one cannot distinguish two separate bands in the data.

The parameters used in calculating the fits to the data are shown in Table III. Note that the fitted doping levels are reasonably close to those we believed present before doing the tunneling experiment. The parameter $2\Delta(0,0)/kT_{c0}$ of the alloy was varied so that the cusp at $|\Delta_1-\Delta_2|/e$ and main peak at $(\Delta_1+\Delta_2)/e$ occurred at the voltages indicated by the data, where $\Delta(0,0)$ is the order parameter for the alloy at zero concentration and at $T=0$ K; T_{c0} is the transition temperature for the undoped alloy. Since T_{c0} is not known, it was adjusted, and therefore the concentration (c) was adjusted, so as to give the Mn-associated structure approximately the observed shape and size.

Kunz and Ginsberg[11] have calculated the values of ϵ_l for various alloys from band theory. They considered four possible configurations for the spins of the electrons of the Mn atom in Zn. For each configuration, they calculated a set of ϵ_l's ($l=0,1,2$), and for each set of ϵ_l they found dT_c/dc. Their value of dT_c/dc that is closest to the experimental value is -104 K/at.%, and the DOS corresponding to this value contains the band of states which is located lowest in energy. We have calculated the conductance from the DOS (with $\epsilon_0=0.951$, $\epsilon_1=0.842$,

TABLE III. Zn and Zn-Mn fitting parameters.

	Zn Quench-condensed	Zn Annealed	Zn-Mn Quench-condensed	Zn-Mn Annealed
BCS				
T_{c0} (K)	1.524	1.060	1.442	
$\Delta(0,0)/kT_{c0}$	1.597	1.760	1.70	
c (at. ppm)	0	0	0	
σ (meV)	0.0066	0.0102	0.0185	
DOS I				
T_{c0} (K)		1.063	1.473	1.000
$\Delta(0,0)/kT_{c0}$		1.750	1.676	1.800
c (at. ppm)		0.1	1.08	1.08
σ (meV)		0.0085	0.0165	0.08
DOS II				
T_{c0} (K)		1.063	1.483	1.01
$\Delta(0,0)/kT_{c0}$		1.750	1.676	1.800
c (at. ppm)		0.09	1.23	1.23
σ (meV)		0.009	0.0165	0.08

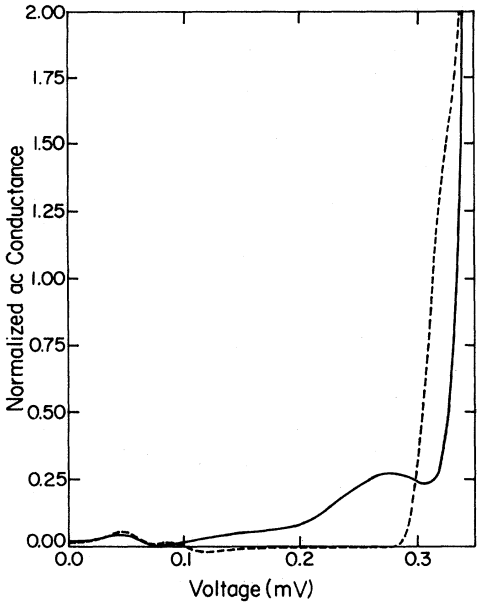

FIG. 7. Solid curve shows the low-bias-voltage region of the experimental ac conductance for the annealed Zn-Mn sample. The dashed line shows the conductance calculated from a set of ϵ_l's found from band-theory calculations.

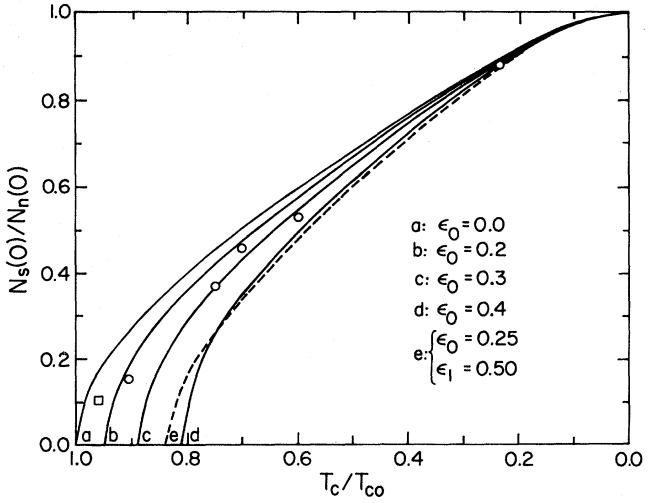

FIG. 8. Comparison of Smith's critical field data with Shiba's theory. The solid curves (from Ref. 18) show the DOS at zero energy in Shiba's theory, using s-wave scattering only, for several values of ϵ_0, as a function of reduced transition temperature. The dashed line shows the DOS at zero energy in Shiba's theory for the set of ϵ_l's used in DOS II of Fig. 4, as a function of reduced transition temperature. The circles are values of γ^*/γ as measured by Smith. The square is the DOS at zero energy as deduced from our tunneling data for the annealed Zn-Mn (1 at. ppm) sample.

$\epsilon_2=0.998$), using $T_{c0}=1.01$ K (as used for DOS II), and we show it in Fig. 7 along with our measured conductance for the annealed Zn-Mn sample. This conductance does not fit our data as well as that calculated from our chosen DOS.

All of the theoretical conductances which we have shown have been smeared by us, using a Gaussian smearing function, so that the theoretical conductance at the peak near $(\Delta_1+\Delta_2)/e$ matches the experimental value. The smeared conductance $f(x)$ is given by

$$f(x_0)=\frac{1}{\sigma\sqrt{\pi}}\int_{-\infty}^{\infty} y(x)\exp\left[-\left[\frac{x-x_0}{\sigma}\right]^2\right]dx\ ,$$

where $y(x)$ is the calculated conductance. (Similar smearing of the peak height has been seen in almost all other published SIS tunneling curves.) The halfwidth of the Gaussian, σ, used in each fit is given in Table III. Even with this smearing, however, the experimentally observed band of states is broader than that predicted by theory. In the data for the quench-condensed samples, the band is so broad that it cannot be resolved. (We have also tried smearing the theoretical curves from our previous experiments,[1,2] and find that the observed bands are broader than the smeared theoretical bands.)

Our results on the annealed films can be compared with published data obtained for bulk samples. Smith[7] has measured the critical field of Zn-Mn samples and calculated the linear coefficient of temperature in the electronic specific heat, γ^*, from his data. The coefficient γ^* should be proportional to the density of electron states at the Fermi energy. Shiba[18] has compared Smith's values of γ^*/γ, where γ is the normal-state coefficient of pure Zn, to the values of $N_s(0)/N_n(0)$ calculated for s-wave scattering only. We have calculated $N_s(0)/N_n(0)$ for the set of ϵ_l's used in the DOS II of Fig. 4, and we show the result in Fig. 8. Comparing Smith's data with our calculation, it is clear that $N_s(0)/N_n(0)$ for DOS II is too small to be consistent with Smith's data. This shortage of states in DOS II at zero energy can also be seen in our data (Fig. 2), since the measured conductance at $V=\Delta_2/e\cong 0.210$ mV is larger than the calculated conductance. (At a bias voltage equal to the aluminum energy gap, all of the conductance is due to the DOS at zero energy in the sample film.) This indicates that Zn-Mn has a larger DOS at zero energy than that shown in our calculated DOS. We have estimated $N_s(0)/N_n(0)$ from our data by adding a constant to the second DOS in Fig. 4, making the calculated and measured conductances agree at $V=\Delta_2/e$. This value of $N_s(0)/N_n(0)$ is shown in Fig. 8, and agrees reasonably well with Smith's data.

It should be noted that the theory of Shiba and Rusinov, to which we have compared our results, treats the spin of the magnetic atom classically. A quantum-mechanical treatment of the spin, as given by the theory of Müller-Hartmann and Zittartz[19] (MHZ) is necessary if one is to include the Kondo effect. It is well known[20] that Zn-Mn is a Kondo alloy, with a Kondo temperature ~ 0.25 K. It would therefore be of great interest to compare our data with predictions of the MHZ theory (which we involved in discussing earlier data from our group on the specific heat of In-Mn and In-Cr alloys[21]). Unfortunately, the MHZ theory in its present form includes only s-wave scattering, and it is known[22] that one needs to include the scattering of higher partial waves if one wishes to treat an alloy system like Zn-Mn, in which T_c decreases

so rapidly with increasing concentration of the magnetic dopant atoms. The electronic density of states predicted by the MHZ theory has a band of the same shape as that predicted by the Shiba-Rusinov theory when only *s*-wave scattering is taken into account. It may be true that the two theories would predict bands of the same shape when the higher partial waves are included, but this remains to be shown.

IV. CONCLUSIONS

We conclude that the doping of Zn with a small concentration of Mn introduces the theoretically expected states into the energy gap. Our results can be explained qualitatively by using Shiba and Rusinov's theory. The band of states seen in the annealed Zn-Mn is well defined but broader than that predicted by theory, and there is a larger DOS at zero energy than predicted. The DOS at zero energy estimated from our data agrees reasonably well with that determined from Smith's[7] critical field measurements on bulk Zn-Mn. The smearing of the bands of states has been seen in other tunneling experiments.[1–4] The excessive width of the bands may be due to the magnetic atoms existing in more than one atomic configuration in the alloy. On the other hand, the theory may not account for the bound-state width properly. The conductance of the quench-condensed film shows not a well-defined band of states, but rather a broad background of states, probably because of local disorder.

ACKNOWLEDGMENTS

This work was supported in part by the Materials Science Division of the U.S. Department of Energy under Contract No. DE-AC02-76ER01198. We are grateful to John B. Woodhouse for performing the electron and optical microscopy measurements for us.

---

*Present address: Argonne National Laboratory, Argonne, IL 60439.

[1]J.-K. Tsang and D. M. Ginsberg, Phys. Rev. B 21, 132 (1980).
[2]J.-K. Tsang and D. M. Ginsberg, Phys. Rev. B 22, 4280 (1980).
[3]B. D. Terris and D. M. Ginsberg, Phys. Rev. B 25, 3132 (1982).
[4]W. Bauriedl, P. Ziemann, and W. Buckel, Phys. Rev. Lett. 47, 1163 (1981).
[5]M. Hansen, *Constitution of Binary Alloys* (McGraw-Hill, New York, 1958).
[6]H. Falke, H. P. Jablonski, J. Kastner, and E. F. Wassermann, Z. Phys. 259, 135 (1973).
[7]F. W. Smith, J. Low. Temp. Phys. 5, 683 (1971).
[8]H. Shiba, Prog. Theor. Phys. 40, 435 (1968).
[9]A. I. Rusinov, Zh. Eksp. Teor. Fiz. 56, 2047 (1969) [Sov. Phys.—JETP 29, 1101 (1969)].
[10]D. M. Ginsberg, Phys. Rev. B 20, 960 (1979).
[11]A. B. Kunz and D. M. Ginsberg, Phys. Rev. B 22, 3165 (1980).
[12]Material obtained from A. D. MacKay, Darien, Connecticut.
[13]Material obtained from Americal Smelting and Refining Company.
[14]J. B. Woodhouse (private communication).
[15]B. W. Roberts, J. Phys. Chem. Ref. Data 5, 581 (1976).
[16]A. C. Thorsen, T. Wolfram, and L. E. Valby, Phys. Lett. 25A, 548 (1967).
[17]*American Institute of Physics Handbook,* 3rd. ed. (AIP, New York, 1972).
[18]H. Shiba, Prog. Theor. Phys. 50, 50 (1973).
[19]E. Müller-Hartmann, in *Magnetism,* edited by H. Suhl (Academic, New York, 1973), Vol. V, p. 353.
[20]R. S. Newrock, B. Serin, J. Vig, and G. Boato, J. Low Temp. Phys. 5, 701 (1971).
[21]B. C. Gibson, D. M. Ginsberg, and P. C. L. Tai, Phys. Rev. B 19, 1409 (1979).
[22]D. M. Ginsberg, Phys. Rev. B 10, 4044 (1974).